

**Biophysical Journal, Volume 121**

**Supplemental information**

**Feedback-controlled dynamics of neuronal cells on directional surfaces**

**Marc Descoteaux, Jacob P. Sunnerberg, Donovan D. Brady, and Cristian Staii**

## **Text S1:**

### **Surface preparation and cell culture**

To fabricate micro-patterned substrates we start with 20mL polydimethylsiloxane (PDMS) solution (Silgard, Dow Corning) with a mixing ratio silicone base/curing agent 15:1 (15 Sylgard 184 silicone elastomer base to 1 Sylgard 184 silicone elastomer curing agent). The PDMS solution is poured over diffraction gratings with slit separations: 1  $\mu\text{m}$  - 10  $\mu\text{m}$  (in increments of 1  $\mu\text{m}$ ) and total surface area 25 x 25 mm<sup>2</sup> (Scientrific Pty. and Newport Corp. Irvine, CA). The PDMS films were left to polymerize for 48 hrs at room temperature, then peeled away from the diffraction gratings and cured at 55<sup>0</sup> C for 3 hrs. We use AFM imaging to ensure that the pattern was successfully transferred from the diffraction grating to the PDMS surface (Fig. 1 *a* and Fig. S1 *a*). The result is a series of periodic patterns (parallel lines with crests and troughs) with constant distance  $d$  between two adjacent lines. The AFM images in Fig. 1 and Fig. S1 show that the patterns are periodic and have constant depth. The surfaces were then glued to glass slides using silicone glue and dried for 48 hours. Next, each surface was cleaned with sterile water and spin-coated with 3 mL of Poly-D-lysine (PDL) (Sigma-Aldrich, St. Louis, MO) solution of concentration 0.1 mg/mL. The spinning was performed for 10 minutes at 1000 RPM. Prior to cell culture the surfaces have been sterilized using ultraviolet light for 30 minutes.

Cortical neurons have been obtained from rat embryos (day 18 embryos obtained from Tufts Medical School). The brain tissue protocol was approved by Tufts University Institutional Animal Care Use Committee and complies with the NIH guide for the Care and Use of Laboratory Animals. The cortices have been incubated in 5 mL of trypsin at 37°C for 20 minutes. To inhibit the trypsin we have used 10 mL of soybean trypsin inhibitor (Life Technologies). Next, the neuronal cells have been mechanically dissociated, centrifuged, and the supernatant was removed.

After this step the neurons have been re-suspended in 20 mL of neurobasal medium (Life Technologies) enhanced with GlutaMAX, b27 (Life Technologies), and pen/strep. Finally, the neurons have been re-dispersed with a pipette, counted, and plated on PDL coated glass, or PDL coated PDMS substrates, at a density of 4,000 cells/cm<sup>2</sup>. Fig. S1 *b* shows the average value for the surface roughness measured on micropatterned PDMS surfaces with spatial periods considered in this paper ( $d$  in the range 1 – 10  $\mu\text{m}$ ). These values are measured before (blue data points) and after (red data points) each surface is coated with PDL. The variation of the average roughness among these substrates is less than 10%. Fig. S2 shows an example of an AFM force map image used to measure the substrate elastic modulus. Fig. S3 shows examples of histograms for the distribution of elastic modulus  $E$ , which are obtained from AFM force maps measured, respectively, before (Fig. S3 *a*) and after (Fig. S3 *b*) coating of the PDMS substrate with PDL. The two histograms display similar ranges for  $E$ , while the corresponding values for the average elastic modulus differs by only 5% between the two maps. The experimental data thus demonstrates that the surface topography and elastic modulus does not vary significantly among the micropatterned PDMS surfaces with different spatial periods  $d$ .

## **Text S2:**

### **Fluorescence and AFM imaging**

For fluorescence imaging the cortical neurons cultured on glass or PDMS surfaces, were rinsed with phosphate buffered saline (PBS) and then incubated for 30 minutes at 37°C with 50 nM Tubulin Tracker Green (Oregon Green 488 Taxol, bis-Acetate, Life Technologies, Grand Island, NY) in PBS. The samples were then rinsed twice with PBS and re-immersed in PBS solution for imaging. Fluorescence images were acquired using a standard Fluorescein

isothiocyanate -FITC filter: excitation of 495 nm and emission 521 nm. Axon outgrowth was tracked using ImageJ (National Institute of Health). To obtain the angular distributions (Fig. 3, Fig. 4 and Fig. S6) all axons have been tracked and then partitioned into segments of 20  $\mu\text{m}$  in length. We have then recorded the angle that each segment makes with the  $x$  axis (Fig. 1), and the results were plotted as angular histograms (Figs. 3, 4 and S6). All surfaces were imaged using an MFP3D Atomic Force Microscope (AFM), equipped with a BioHeater closed fluid cell, and an inverted Nikon Eclipse Ti optical microscope (Micro Video Instruments, Avon, MA). The AFM topographical images of the surfaces were obtained using the AC mode of operation, and AC 160TS cantilevers (Asylum Research, Santa Barbara, CA). Surfaces were imaged both before and after neuronal culture, and no significant change in topography was observed.

**Text S3:**

**Simulations of growth cone trajectories**

We perform simulations of growth cone trajectories using the stochastic Euler method with  $N$  steps (26,27). With this method the change in position of the growth cone and the turning angle at each step are parametrized by the arclength  $s$  from the axon's initial position:

$$\Delta x(s) = \cos(\theta) \cdot \Delta s$$

$$\Delta y(s) = \sin(\theta) \cdot \Delta s$$

$$\Delta\theta(s) = -\gamma \cdot \cos(\theta) + D \cdot dW$$

where  $-\gamma \cdot \cos(\theta)$  is a deterministic steering torque (12, 18), and  $D \cdot dW$  is an uncorrelated Wiener process representing the randomness in the axon steering ( $\gamma$  and  $D$  represent the damping and diffusion coefficients, respectively, which are defined in the main text, see Eq. 2). The angle  $\theta$  is determined from the spatial probability distribution, which is the solution of the Fokker-Planck

(Eq. 2 and Eq. 7 in the main text). The velocity distributions are obtained from the change in position of the growth cone at each step (26,27).

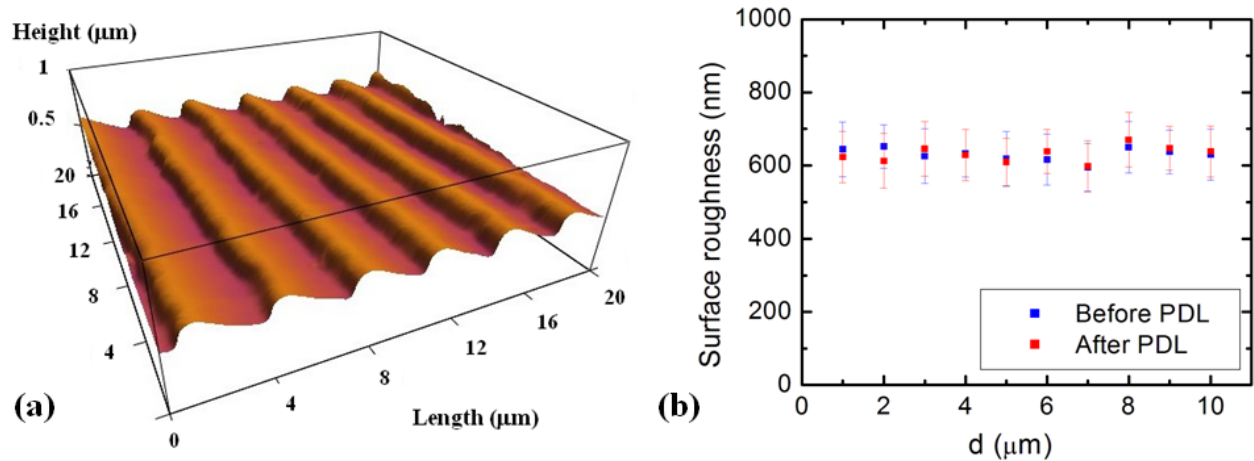


**FIGURE S1.** (a) Atomic Force Microscope (AFM) topographic image of a PDL coated PDMS micropatterned surface. The image shows that the micropatterns have a periodic profile, with a spatial period  $d = 4 \mu\text{m}$ , and a constant depth of approximately  $0.6 \mu\text{m}$ . (b) Variation of the surface roughness on micropatterned PDMS surfaces with spatial periods considered in this paper ( $d$  in the range  $1 - 10 \mu\text{m}$ ). The surface roughness is measured with the AFM. The blue data points show the average surface roughness measured before PDL coating. The red data points show the average surface roughness measured on the same surfaces after coating with PDL. The error bars indicate the standard error of the mean. The data demonstrates that the surface roughness does not vary significantly among the PDMS surfaces with different spatial periods  $d$ , and it does not change significantly upon surface coating with PDL. The variation of the average roughness among these substrates is less than 10%.

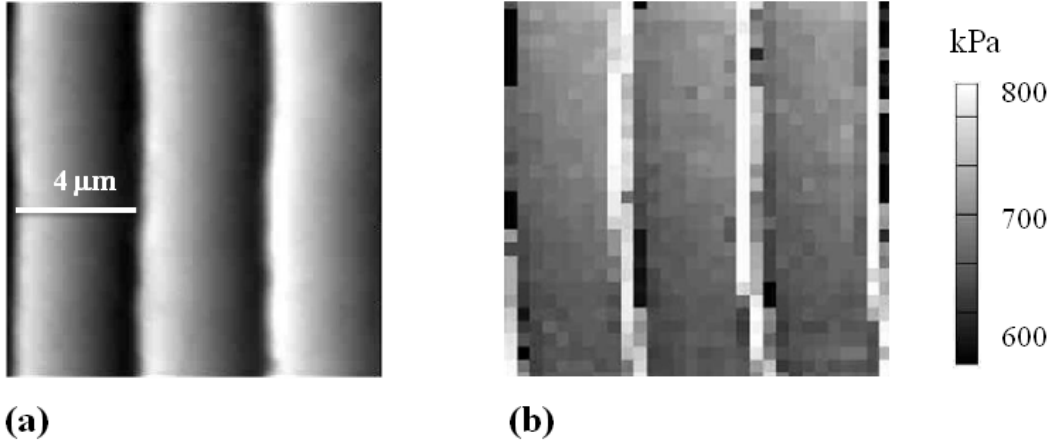


**FIGURE S2.** Examples of (a) AFM topographic image, and (b) AFM force map image measured on a micropatterned PDMS surface coated with PDL. Each pixel corresponds to a value of the elastic modulus. The maps for the elastic modulus are measured following the procedure presented in detail in references (41) and (42). The scale bar shown in (a) is the same for both images.

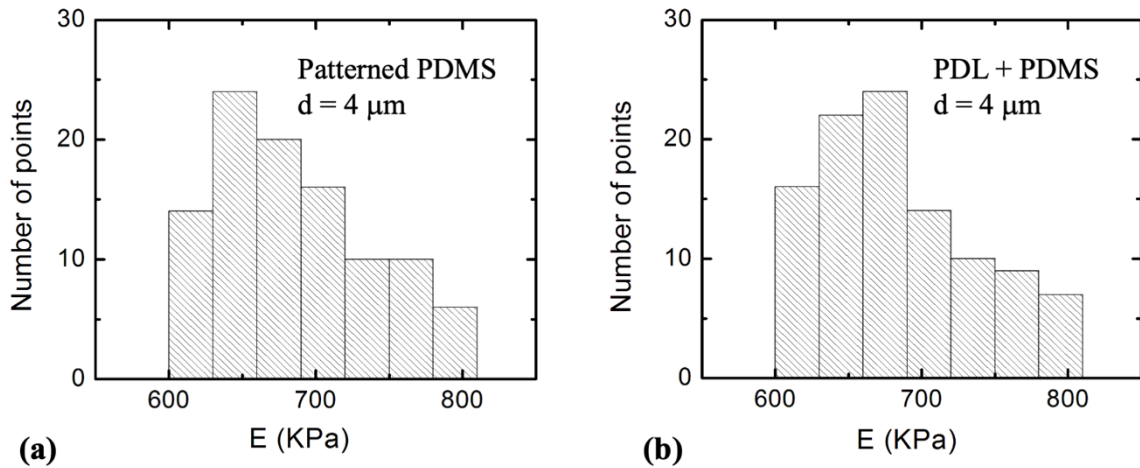


**FIGURE S3.** Examples of histograms for the substrate elastic modulus  $E$  measured from AFM force maps shown in Fig. S2. (a) Histogram for elastic modulus for a PDMS surface with  $d = 4 \mu\text{m}$ , measured before coating the surface with PDL. (b) Histogram for elastic modulus for the same PDMS surface shown in (a), measured after coating the surface with PDL. The two maps display similar ranges for  $E$ . The average elastic modulus between the two maps differs by only

5%. The data demonstrates that PDL coating does not change the elastic modulus of the PDMS substrate.



**FIGURE S4.** Examples of tracked positions for two axons. The segments marked in yellow are superimposed on the axon and show the growth trajectory. The numbers on each segment represent different positions of the growth cone during growth. The locations of the corresponding micropatterns are shown by the dotted blue lines. Each segment is 20  $\mu\text{m}$  in length as described in the Data Analysis section in the main text.

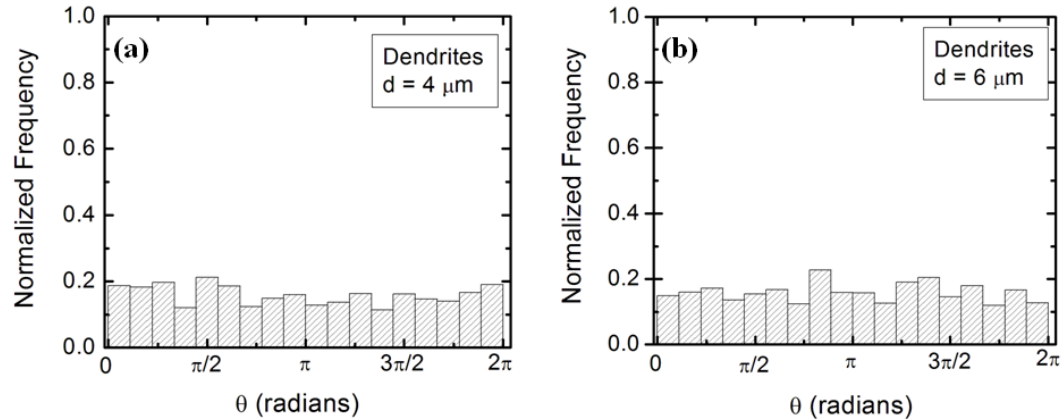


**FIGURE S5.** Examples of normalized experimental angular distributions for dendrites growth measured on micropatterned PDMS surfaces with different pattern spatial periods. The vertical axis (labeled Normalized Frequency) represents the ratio between the number of dendrite segments growing in a given direction and the total number  $N$  of axon segments. Each dendrite segment is of  $20 \mu\text{m}$  in length. All distributions show data collected at  $t = 40$  hrs after neuron plating. (a) Angular distribution obtained for  $N = 647$  different dendrite segments on surfaces with  $d = 4 \mu\text{m}$ . (b) Angular distribution obtained for  $N = 720$  different dendrite segments on surfaces with  $d = 6 \mu\text{m}$ . The data shows that, in contrast to axons, the dendrites do not display directional alignment along the surface micropatterns.



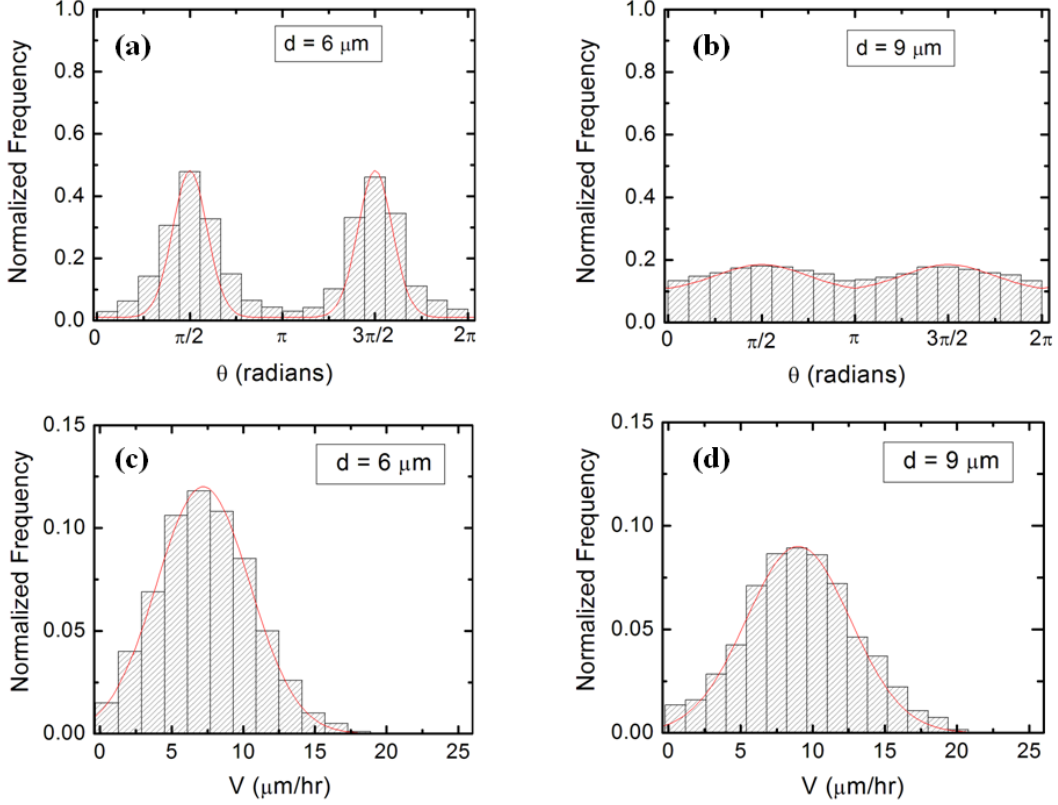


**FIGURE S6.** (a-b) Examples of normalized experimental angular distributions for axonal growth for untreated neurons measured on micropatterned PDMS surfaces with different pattern spatial period  $d$ . The continuous red curves in each figure are the predictions of the theoretical model (see the main text). The vertical axis (labeled Normalized Frequency) represents the ratio between the number of axonal segments growing in a given direction and the total number  $N$  of axon segments. Each axonal segment is of  $20 \mu\text{m}$  in length (see section on data analysis in the main text). All distributions show data collected at  $t=40$  hrs after neuron plating. (a) Angular distribution obtained for  $N = 1328$  different axon segments on surfaces with  $d = 6 \mu\text{m}$ . (b) Angular distribution obtained for  $N = 1261$  different axon segments on surfaces with  $d = 9 \mu\text{m}$ . The data shows that the axons display strong directional alignment along the surface patterns (peaks at  $\theta = \pi/2$  and  $\theta = 3\pi/2$ ), with the high degree of alignment (sharpness of the distribution) measured for  $d = 6 \mu\text{m}$ . The degree of alignment is greatly reduced for neuronal growth on surfaces with  $d = 9 \mu\text{m}$ . (c-d)

Examples of normalized speed distributions for growth cones measured on micropatterned PDMS surfaces with different pattern spatial period  $d$ . (c) Speed distribution for  $N = 305$  different growth cones measured on surfaces with  $d = 6 \mu\text{m}$ . (d) Speed distribution for  $N = 285$  different growth cones measured on surfaces with  $d = 9 \mu\text{m}$ . The continuous red curves in each figure represent the predictions of the theoretical model discussed in the main text.

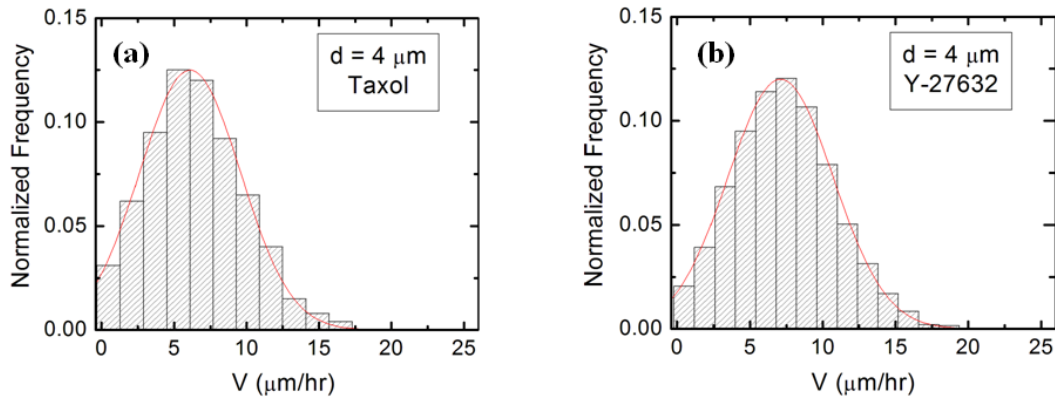


**FIGURE S7.** Examples of normalized speed distributions obtained for growth cones of cortical neurons treated with chemical compounds that inhibit the cytoskeletal dynamics. The growth substrates are PDL coated PDMS surfaces with periodic micro-patterns with the pattern spatial  $d = 4 \mu\text{m}$ . The images are captured at  $t = 40$  hrs after neuron plating. (a) Speed distribution measured for  $N = 274$  different growth cones for neurons treated with Taxol (inhibitor of microtubule dynamics). (d) Speed distribution measured for  $N = 256$  different growth cones for neurons treated with Y-27632 (inhibitor of actin dynamics). The continuous red curves in each figure represent the predictions of the theoretical model discussed in the main text.

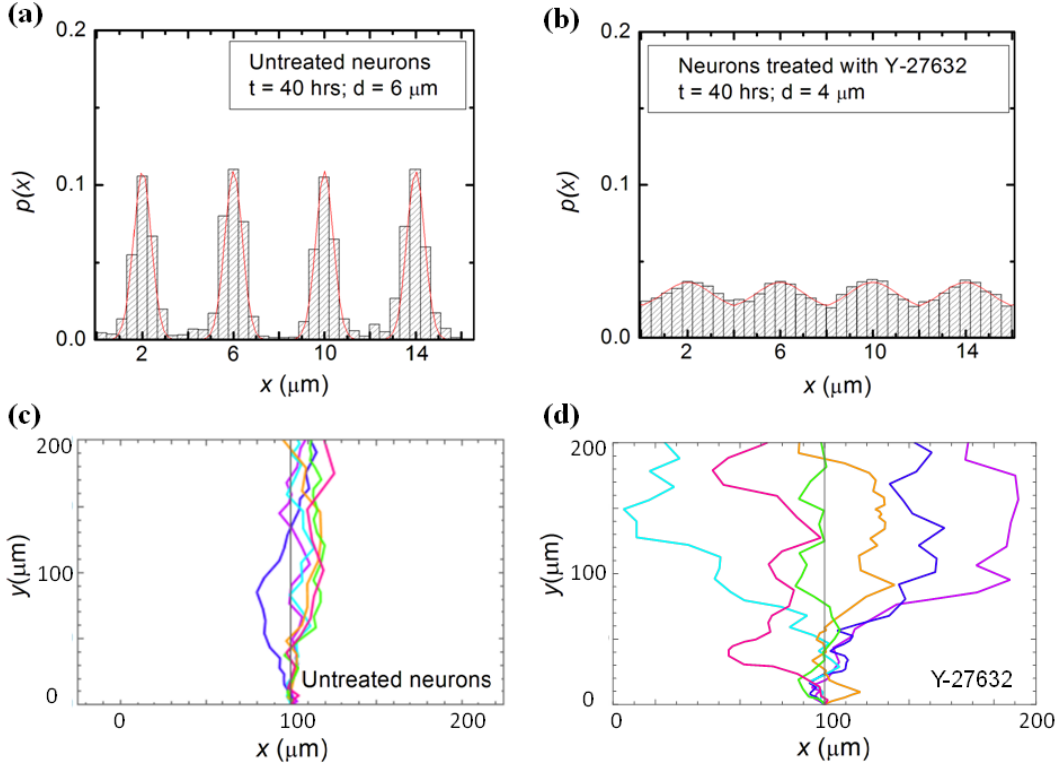


**FIGURE S8.** (a-b) Examples of experimentally measured probability distributions for the motion of the growth cone in the  $x$  direction. The red curves represent fits to the data with the solutions of the theoretical model given by Eq. 7. The fit parameters are the diffusion (cell motility) coefficient  $D$ , the damping coefficient  $\gamma$ , and the magnitudes  $V_0$  and  $V$  of the external and feedback potential, respectively. (a) Data obtained for  $N = 341$  untreated neurons measured at  $t = 40$  hrs on PDMS surfaces with  $d = 4 \mu\text{m}$ . (b) Data obtained for  $N = 316$  neurons treated with Y-27632 measured at  $t = 40$  hrs on PDMS surfaces with  $d = 4 \mu\text{m}$ . (c-d) Simulated neuronal growth for untreated (c) and Y-27632 - treated neurons (b). The simulations are performed by using the values of the growth parameters obtained from the fit of the experimental data with solutions of Eq. 7 (seen main text).

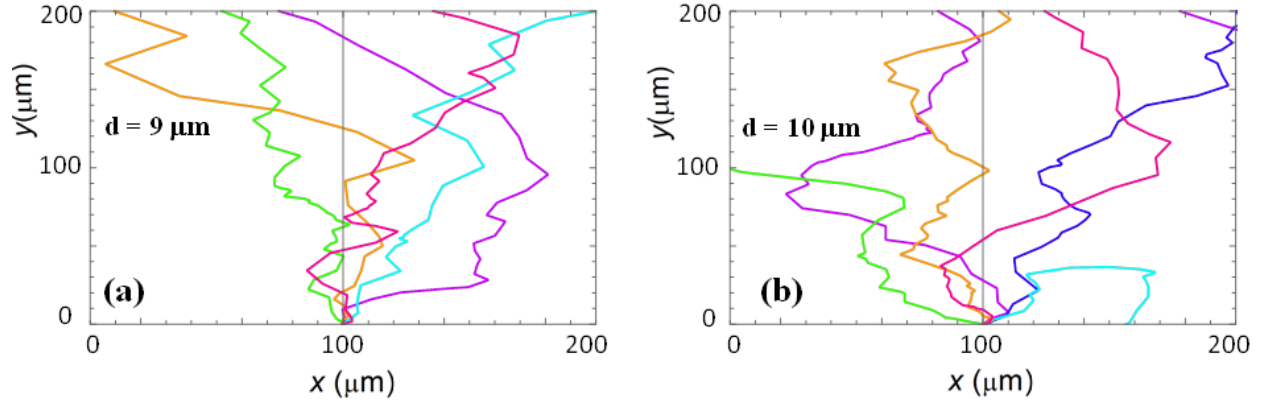


**FIGURE S9.** Example of simulated axonal growth for untreated neurons cultured on PDMS surfaces with relatively large spatial periods: (a):  $d = 9 \mu\text{m}$  and (b):  $d = 10 \mu\text{m}$ . The axons display a low degree of alignment, in agreement with the experimental observations (see Fig. S6 *b* and reference (21)). The simulations are performed by using the values of the growth parameters obtained from the fit of the experimental data with solutions of Eq. 7 (seen main text).

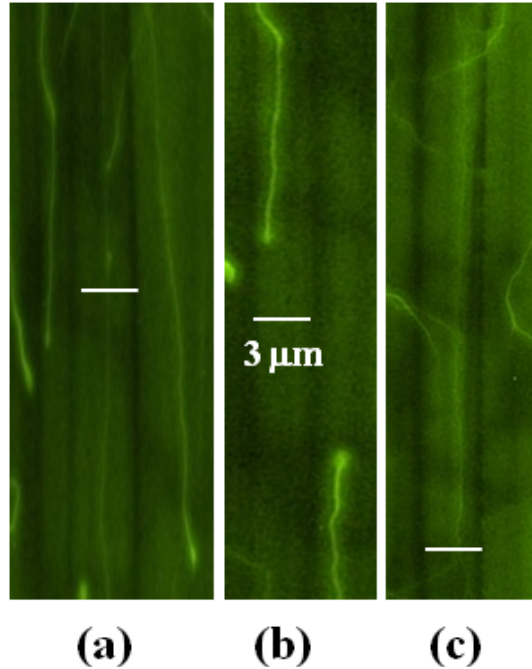


**FIGURE S10.** Examples of fluorescence images showing the position of axons with respect to the patterns. The images have been taken using the high magnification objective (60x) of the Nikon Eclipse Ti microscope, at different locations on 3 different PDMS substrates. The images show the fluorescently labeled microtubules (green), i.e. the C domain (see reference (1, 2)) inside the axons. The microtubules are labeled using Tubulin Tracker Green (see main text). The position of the micro-patterned troughs is shown by the vertical black lines. The 3 $\mu\text{m}$  white scale bar shows the distance between two adjacent troughs, and it has the same size for all images. The images show that the axons are located on the ridges of the patterns. The position of the ridges and troughs has been verified using AFM (images similar to the one shown in Fig. 1 *a* and Fig. S1 *a*).

Cell/ Substrate	$D(\mu\text{m}^2/\text{hr})$	$\gamma(\text{hr}^{-1})$	$V_0(\mu\text{m}^2/\text{hr}^2)$	$V(\text{hr}^{-2})$	$\alpha(\mu\text{m})^{-1}$	$B/E_0(\mu\text{m}^2)$
Untreated $d=1\ \mu\text{m}$	$19 \pm 2$	$0.13 \pm 0.04$	$1.4 \pm 0.5$	$0.18 \pm 0.05$	$1.9 \pm 0.4$	$7.3 \pm 0.9$
Untreated/ $d=4\ \mu\text{m}$	$22 \pm 4$	$0.14 \pm 0.05$	$1.9 \pm 0.3$	$0.23 \pm 0.08$	$1.9 \pm 0.4$	$7.4 \pm 0.9$
Untreated/ $d=6\ \mu\text{m}$	$21 \pm 3$	$0.15 \pm 0.05$	$2.0 \pm 0.4$	$0.24 \pm 0.08$	$1.9 \pm 0.4$	$7.6 \pm 0.9$
Untreated $d=9\ \mu\text{m}$	$17 \pm 3$	$0.12 \pm 0.05$	$1.1 \pm 0.05$	$0.14 \pm 0.06$	No value	$6.8 \pm 0.9$
Untreated $d=10\ \mu\text{m}$	$16 \pm 3$	$0.10 \pm 0.06$	$0.9 \pm 0.05$	$0.11 \pm 0.06$	No value	$6.8 \pm 0.9$
Taxol $d=4\ \mu\text{m}$	$14 \pm 3$	$0.11 \pm 0.03$	$0.6 \pm 0.2$	$0.08 \pm 0.04$	$0.5 \pm 0.2$	$5.5 \pm 0.9$
Y-27632 $d=4\ \mu\text{m}$	$12 \pm 4$	$0.09 \pm 0.03$	$0.5 \pm 0.03$	$0.06 \pm 0.04$	$0.3 \pm 0.2$	$5.1 \pm 0.9$

**TABLE S1.** Summary of the parameter values for untreated and chemically modified neurons.

The table shows the values for the growth parameters of untreated and chemically modified neuronal cells, grown on different types of micropatterned PDMS substrates. The uncertainty for each parameter represents the uncertainties from the fit of the corresponding data points. The values for the parameter  $\alpha$  are obtained for  $d$  in the range  $d = 1$  to  $6\ \mu\text{m}$ , as discussed in the main text.